Neuropharmacology 95 (2015) 192–205

Contents lists available at ScienceDirect

Neuropharmacology

journal homepage: www.elsevier.com/locate/neuropharm

Cortical oscillatory dynamics and benzodiazepine-site modulation of tonic inhibition in fast spiking interneurons

Emma J. Prokic [a], Cathryn Weston [b], Naoki Yamawaki [a, 1], Stephen D. Hall [a, 2], Roland S.G. Jones [c], Ian M. Stanford [a], Graham Ladds [b, **], Gavin L. Woodhall [a, *]

[a] Aston Brain Centre, Aston University, School of Life and Health Sciences, Birmingham, B4 7ET, UK
[b] Division of Biomedical Cell Biology, University of Warwick Medical School, Coventry, CV4 7AL, UK
[c] Department of Pharmacology, University of Bath, Claverton Down, Bath, BA2 7AY, UK

ARTICLE INFO

Article history:
Received 25 November 2014
Received in revised form
9 February 2015
Accepted 8 March 2015
Available online 20 March 2015

Keywords:
$GABA_A$ receptors
Beta oscillations
Tonic current
Zolpidem
Fast spiking interneurons
Motor cortex

ABSTRACT

Tonic conductance mediated by extrasynaptic $GABA_A$ receptors has been implicated in the modulation of network oscillatory activity. Using an *in vitro* brain slice to produce oscillatory activity and a kinetic model of $GABA_A$ receptor dynamics, we show that changes in tonic inhibitory input to fast spiking interneurons underlie benzodiazepine-site mediated modulation of neuronal network synchrony in rat primary motor cortex. We found that low concentrations (10 nM) of the benzodiazepine site agonist, zolpidem, reduced the power of pharmacologically-induced beta-frequency (15–30 Hz) oscillatory activity. By contrast, higher doses augmented beta power. Application of the antagonist, flumazenil, also increased beta power suggesting endogenous modulation of the benzodiazepine binding site. Voltage-clamp experiments revealed that pharmacologically-induced rhythmic inhibitory postsynaptic currents were reduced by 10 nM zolpidem, suggesting an action on inhibitory interneurons. Further voltage-clamp studies of fast spiking cells showed that 10 nM zolpidem augmented a tonic inhibitory $GABA_A$ receptor mediated current in fast spiking cells whilst higher concentrations of zolpidem reduced the tonic current. A kinetic model of zolpidem-sensitive $GABA_A$ receptors suggested that incubation with 10 nM zolpidem resulted in a high proportion of $GABA_A$ receptors locked in a kinetically slow desensitized state whilst 30 nM zolpidem favoured rapid transition into and out of desensitized states. This was confirmed experimentally using a challenge with saturating concentrations of GABA. Selective modulation of an interneuron-specific tonic current may underlie the reversal of cognitive and motor deficits afforded by low-dose zolpidem in neuropathological states.

1. Introduction

The primary motor cortex (M1) exhibits neuronal network oscillatory activity at beta frequency (15–30 Hz) (Murthy and Fetz, 1992; Baker et al., 1997). The power of this oscillatory activity is dynamic, changing with the anticipation, initiation and termination of movement (Cheyne et al., 2008). Loss of dynamicity through excessive synchronization and raised oscillatory power may underlie deficits associated with Parkinson's disease (Brown, 2003; Brown et al., 2004; Kuhn et al., 2006). Similarly, other neuropathologies involve altered oscillatory activity, including stroke (Tecchio et al., 2006; Hall et al., 2010), Alzheimer's disease (Poza et al., 2007) and schizophrenia (Canive et al., 1996; Ford et al., 2007).

As with gamma (35–80 Hz) oscillations (Whittington et al., 1995; Traub et al., 1996), beta oscillatory activity in M1 is generated as a consequence of sustained excitation of networks of inhibitory interneurons (Yamawaki et al., 2008). Inhibitory interneurons are able to entrain each other to fire in a synchronous manner and hence sculpt pyramidal cell activity through repetitive (phasic) inhibitory discharges, the frequency of which is dependent

Abbreviations: AHP, after-hyperpolarization; aCSF, artificial cerebrospinal fluid; CCh, carbachol; FS, fast spiking; I_{tonic}, tonic inhibitory current; M1, primary motor cortex; IEI, interevent interval; IPSCs, inhibitory postsynaptic currents; KA, kainic acid; KS, Kolmogorov–Smirnov test; LFP, local field potential; ODEs, ordinary differential equations; sIPSCs, spontaneous IPSCs.

* Corresponding author. Tel.: +44 121 204 3995.
** Corresponding author. Tel.: +44 247 615 0220.
E-mail addresses: Graham.Ladds@warwick.ac.uk (G. Ladds), G.L.Woodhall@aston.ac.uk (G.L. Woodhall).
[1] Northwestern University, Chicago, USA.
[2] School of Psychology, Plymouth University, UK.

http://dx.doi.org/10.1016/j.neuropharm.2015.03.006

upon the kinetics of the inhibitory postsynaptic potentials (Whittington et al., 1995; Fisahn et al., 1998; Traub et al., 2003). Recent evidence suggests that a sustained inhibitory membrane conductance (I_{tonic}), arising from spillover of GABA, and mediated by high affinity extrasynaptic $GABA_A$ receptors (Farrant and Nusser, 2005; Bright et al., 2007) also plays a fundamental role in shaping network excitability (Semyanov et al., 2004; Mann and Mody, 2010). In thalamus (Belelli et al., 2005; Cope et al., 2005; Bright et al., 2007), dentate gyrus (Nusser and Mody, 2002) and cerebellum (Brickley et al., 1996), I_{tonic} is maintained by the activity of GABA receptors containing benzodiazepine insensitive ∂ and/or α4 or α6 subunits (Brickley et al., 2001). However, I_{tonic} may also be mediated by receptors containing the α5 and ∂ subunits (Clarkson et al., 2010). In addition, a benzodiazepine-sensitive, presumably non-∂ subunit mediated I_{tonic} has been reported in hippocampal neurons (Bai et al., 2001; Semyanov et al., 2003, 2004) and somatosensory cortex (Yamada et al., 2007). As I_{tonic} is more active in fast-spiking (FS) interneurons compared to pyramidal cells (Semyanov et al., 2003), and FS cells have been reported to express high levels of α1 subunit containing $GABA_A$ receptors (Bacci et al., 2003; Thomson et al., 2000), an effect of benzodiazepines on I_{tonic} in a single FS cell could have a profound effect on synchronous activity in neuronal networks.

Using magnetoencephalographic techniques we have recently shown that cognitive and motor deficits in stroke patients are associated with slow wave (4–12 Hz) and beta (15–30 Hz) activity in cortical regions, including M1 (Hall et al., 2010, 2014). Subsedative doses of zolpidem reduce these, correlating with improved clinical outcomes (Hall et al., 2010, 2014). Similarly, in Parkinson's patients, we have shown that the power of interhemispheric beta oscillations is unbalanced compared to controls, such that beta power contralateral to Parkinsonian symptoms is raised above ipsilateral beta power. The imbalance is reversed by sub-sedative doses of zolpidem (Hall et al., 2014) through simultaneous augmentation and depression of contralateral and ipsilateral beta power, respectively. These observations suggest that zolpidem is capable of bidirectional modulation of neuronal network activity *in vivo*. Here, using an *in vitro* brain slice model of neuronal oscillatory activity and a kinetic model of $GABA_A$ receptor dynamics, we show that changes in tonic inhibitory input to FS interneurons produce bidirectional modulation of neuronal network synchrony in M1 mediated by benzodiazepine-site activation.

2. Materials and methods

2.1. Ethical approval

All procedures were approved by Aston University's Local Ethical Review Panel and conducted in accordance with the Animals (Scientific Procedures) Act 1986 UK and European Communities Council Directive 1986 (86/609/EEC).

2.2. Preparation of brain slices

Brain slices were prepared from male Wistar rats (40–60 g). Rats were anaesthetized with isoflurane and transcardially perfused with ice-cold artificial cerebrospinal fluid (aCSF; 100 ml) containing (in mM) sucrose (171), KCl (2.5), $MgCl_2$ (10), $NaHCO_3$ (25), 1.25 NaH_2PO_4, glucose (10), $CaCl_2$ (0.5), ascorbic acid, 2 N-acetyl cysteine (1), taurine (1) and pyruvate (20), and saturated with carbogen gas (95% O_2/5% CO_2), at pH 7.3 and 310 mOsm. Indomethacin (45 μM), a cyclo-oxygenase inhibitor was added to the aCSF to improve cell viability (Pakhotin et al., 1997) and the antioxidants ascorbic acid (300 μM) and uric acid (400 μM) added as neuroprotectants.

The brain was removed, placed in ice-cold sucrose-based aCSF of similar composition to that described above, and sagittal slices including M1 (450 μm for extracellular recording, 350 μm for whole-cell recording) were cut at 5 °C, using a HM650 V microslicer and cooling unit (Microm GMBH, Germany). They were stored in an interface chamber (for extracellular recordings) or a submersion chamber (for whole-cell recordings), at room temperature (24 °C), in oxygenated aCSF containing (in mM) NaCl (126), KCl (3), $MgSO_4$ (1.6), $NaHCO_3$ (26), NaH_2PO_4 (1.25), glucose (10), $CaCl_2$, (2).

2.3. Extracellular recordings

For extracellular recordings, slices were transferred to an interface chamber (Scientific System Design Inc, Canada) and continuously perfused (1–2 ml/min) with glucose-based aCSF. The perfusate was maintained at 33–34 °C using a PTC03 proportional temperature controller (Scientific System Design Inc., Canada). Kainic acid (KA, 100 nM) and carbachol (CCh, 5 μM) were added to the perfusate to promote network oscillatory activity. We measured oscillatory power every 5 min and waited until peak power had been within 10% variance for more than 30 min. Typically, stabilization occurred after 60–90 min.

Local field potential (LFP) recordings were made using borosilicate glass micropipettes filled with aCSF (1–3 MΩ; P-97, Sutter instrument Co, USA) and visually positioned in layer V of M1. Signals were recorded and low-pass filtered (200 Hz) using a programmable signal conditioner (CyberAmp 380, Molecular Devices, USA). Oscillatory activity was digitized at 10 kHz using an A-D converter (CED Micro-1401 mk II; Cambridge Electronic Design, UK) and recorded to disk. Spike2 software (CED, UK) was used for all acquisition and analysis.

2.4. Whole-cell recording

Slices were transferred to a submersion recording chamber perfused at 5–7 ml/min with glucose-based aCSF at 32 ± 0.5 °C, on the stage of an Olympus BX51WI microscope. Layer V in M1 was readily identified by the presence of large pyramidal (Betz) cells visualized using infrared video-microscopy with differential interference contrast optics. Whole-cell recordings were made from cells visually identified as non-pyramidal, using borosilicate glass pipettes (3–4 MΩ).

Current clamp recordings were made with an Axopatch 700A amplifier (Molecular Devices, USA) using electrodes filled with a solution containing (in mM); $KMeSO_4$ (130), HEPES (10) EGTA (5), NaCl (4), Mg-ATP (4), Na-GTP (0.4), pH 7.2 at 295 mOsm. Membrane properties of putative FS cells were characterized electrophysiologically using an incremental series of current steps (250 ms, from −400 pA) until threshold for action potential firing was reached.

For voltage-clamp recordings, electrodes were filled with a solution containing (in mM); CsCl (100), HEPES (40), QX-314 (1), EGTA (0.6), $MgCl_2$ (5) TEA-Cl (10), Na-ATP (4,) Na-GTP (0.4) and IEM 1460 (1), titrated with CsOH to pH 7.25 at 295 mOsm. This chloride-based solution allowed the study of inhibitory postsynaptic currents (IPSCs) recorded at −70 mV using an Axopatch 700A amplifier (Molecular Devices, USA). Currents were filtered at 5 kHz using a four-pole Bessel filter and were digitized at 10 KhZ using pClamp version 10.3 (Molecular Devices, USA). Series resistance was measured regularly via the capacitance transient induced during a line-frequency voltage step (5 mV) during recording. Recordings where this changed by >20% were omitted from analysis.

2.5. Data analysis

All data were analysed off-line using Clampfit 10.2 (Molecular Devices, USA), Spike2 (CED, UK) or Mini-Analysis (Synaptosoft, USA). Spontaneous IPSCs (sIPSCs) were analysed using Mini-analysis. The Kolmogorov–Smirnov (KS) test was used to assess changes in the cumulative probability distribution of inter-event intervals (IEI) and Student's t-test was used to assess changes in IEI, decay time and amplitude. To determine the effects of drugs on spontaneous release, 200 consecutive sIPSCs were analysed from each recording in each condition (control *v* drug) and the median value for interval, amplitude or decay calculated prior to finding a mean-median value across multiple recordings.

In experiments involving application of GABA during whole-cell voltage clamp recording, the rate and extent of desensitization of GABA-induced inward currents was calculated by exponential curve fitting, performed using a simplex algorithm combined with a Chebyshev routine.

$$f(t) = \sum_{i=1}^{n} A_i e^{-\frac{t}{\tau_i}} + C$$

The fit solves for the amplitude A, the time constant τ, and the constant y-offset C for each component i. The reduction in current after a long application of GABA was taken as the steady-state level and calculated as a normalized value of the peak current achieved.

For tonic current measurements, to exclude confounding effects of overlapping sIPSCs, the baseline current was measured as described by Nusser and Mody (2002). Briefly, the mean of a 5-ms epoch was taken every 100 ms. The mean and SD of the averaged baseline points were calculated for 10 s (~100 averaged baseline points) at three distinct times of the recordings (periods *A*, *B*, and *C*). Two changes in the baseline current were calculated between the three periods. The first (ΔBL) was the value of the difference during recording periods *A* and *B*, both taken during the control period and reflecting baseline fluctuation. The second (ΔDrug) was the value of the difference during recording periods *C* and *B*, and reflecting drug induced changes to the holding current. The two baseline changes (ΔBL and ΔDrug) were then statistically compared (paired *t*-test).

The frequency–domain method (*Fast fourier transform* (FFT)) was used to generate power spectra of LFP data. Unless otherwise stated, 60 s epochs of sampled data were analysed using Spike 2 (CED, Cambridge, UK). All statistical analyses were

performed using mean peak values, and, unless otherwise stated, it is these values that are reported in the text.

All data are expressed as mean ± S.E.M. and * indicates significance at $P < 0.05$, ** at $P < 0.01$ and *** at $P < 0.001$.

2.6. Source of drugs

Salts and other agents used in preparation of aCSF and electrode solutions were obtained from Sigma (UK) and Fisher (UK). Bicuculline methobromide, gabazine, zolpidem, THIP (4,5,6,7-Tetrahydroisoxazolo[5,4-*c*]pyridin-3-ol) hydrochloride) and flumazenil (8-Fluoro-5,6-dihydro-5-methyl-6-oxo-4*H*-imidazo[1,5-*a*][1,4]benzodiazepine-3-carboxylic acid) were obtained from Tocris, UK. Drugs were initially prepared in stock solutions of 1–10 mM and stored at −20 °C prior to dilution to the final concentration in aCSF immediately before use.

2.7. Modelling of $GABA_A$ receptor dynamics

Kinetic models were extended from previously published models of $GABA_A$ receptor kinetics (Jones and Westbrook, 1995; Jones et al., 1998; Karayannis et al., 2010), and, where possible, we have remained faithful to these. Models were generated as ordinary differential equations (ODEs) using techniques described previously (Croft et al., 2013) and the system solved using Matlab R2013b (Mathsworks) as follows: To simulate pre-incubation of tissue with either zolpidem or ambient GABA, models were allowed to reach steady state ($t_0 = 150$ s). GABA was then rapidly, but not discontinuously, increased to the specified concentration for each experiment. Simulation of $GABA_A$ channels was calculated by measuring the movement of Cl^- into the cell (see reaction scheme, Fig. 10). To provide a comparison with experimental data, we inverted the response measured to mirror changes in tonic current observed within Cl^- loaded neurons. The concentration profile was modelled for 1 mM GABA at time $t_0 + 200$ s. To simulate the effects of adding zolpidem post GABA stimulation, 10 nM zolpidem was added at $t_0 + 250$ s. Where the models previously generated by Jones and Westbrook (1995) have focused upon single channel kinetics, our models used as many of these parameters as possible and then adapted to show the possible mechanisms of the experimental data using Matlab R2013b. The kinetic rate constants for parameters previously determined experimentally were constrained, while the others were allowed to vary as the software required. Initial conditions and reaction rate constants used in the appropriate models are shown in Fig. 10C.

2.8. Model description – GABA

The model described here contains the same unbound state (U) and two transition states (B_1 and B_2) as published by Jones and Westbrook (1995) (see Fig. 10). However, to describe the precise kinetics observed in our experimental data we have modified and extended this model to contain additional open and desensitized states (depicted by the presence of the dotted boxes in Fig. 10). The Jones and Westbrook (1995) model contains two open states (O_1 and O_2) and two desensitized states (D_1 and D_2) both of which occur following GABA binding. Further to this, we have proposed the existence of an additional open (O_0) and desensitized state (D_0) both occurring from the unbound state (U; Wlodarczyk et al., 2013). To remain consistent with the structure of the Jones and Westbrook model we have allowed the single desensitized (D_1) state to transition with the unbound desensitized state (D_0). As with the Jones and Westbrook models, the two-agonist binding sites are assumed to be equal and independent.

2.9. Model description – zolpidem

To account for the actions of zolpidem binding, previous models of the $GABA_A$ receptor kinetics have simply increased the rate with which GABA binds to its receptor (K_{on}). Here, additional parameters have been fitted to ensure good agreement with experimental data (Karayannis et al., 2010). Our initial attempts at using this K_{on} modelling approach proved unsuccessful in reproducing our experimental data shown in Fig. 11. As a consequence, primarily to reflect the non-intuitive data related to the 10 nM zolpidem effect, we have derived a new kinetic model whereby we allow zolpidem to be a reactant in the scheme. Based upon previous studies (Pritchett et al., 1990; McKernan et al., 1995), zolpidem has been shown to bind to $GABA_A$ receptors with higher or lower affinity, depending on subunit expression of the receptors. For simplicity, we have depicted this as a two-state binding event. The first is the higher affinity state (UZ1) and the second, the lower affinity state (UZ2). Consistent with previous work, we assume that the presence of the bound zolpidem decreases the K_{off} rate of GABA binding and increases the apparent frequency of $GABA_A$ receptor channel opening (see Bianchi et al., 2009; Bianchi, 2010; see rate constants Fig 10C). We next assumed that zolpidem binding is effectively irreversible due to its constant presence in the media. Finally, we assume that the kinetic rate of $GABA_A$ channel opening is equal regardless of zolpidem or GABA bound states, although it is well established that the frequency of opening of GABA receptors may be altered by benzodiazepine binding.

The reaction scheme for the zolpidem model is depicted in Fig. 10B. With zolpidem bound to the low affinity site (UZ2), GABA is now able to bind and the channel transitions through the states analogous to that shown for the GABA binding model. Where possible, the rate constants have been conserved between the two models, however, to account for changes in receptor dynamics brought about by the binding of zolpidem, new rate constants were attributed as shown in Fig. 10C.

2.10. Initial conditions and rate constants used in simulating experimental conditions

The initial concentration of species in the model was, U 5 mM, Cl^-_{out} 130 mM, Cl^-_{in} 0.9 mM and ambient GABA 100 nM. Both concentrations of ambient GABA and Cl^-_{out} remained constant through all simulations to reflect experimental conditions. Zolpidem concentrations were varied as stipulated in each simulation. For the majority of simulations 1 mM GABA was used as the simulating ligand unless stated. The rate constants used were *fixed* parameters when simulating experimental conditions.

3. Results

3.1. Involvement of GABA and benzodiazepine binding in beta-oscillations

Previous studies indicate that $GABA_A$ receptors containing $\alpha 1$ and $\gamma 2$ subunits are present on inhibitory interneurons, including FS cells. Since the benzodiazepine-binding site lies at the interface between these subunits, and GABAergic interneurons are subject to cell-type specific GABA tone, we hypothesized that benzodiazepine-site activation would act, via GABAergic interneurons, to modulate oscillatory activity.

We generated persistent oscillations at 'beta' (high beta/low gamma) frequency (Fig. 1A; mean peak frequency 30.1 ± 0.5 Hz; mean power 119.9 ± 16.5 μV^2, n = 128) in slices of M1 by application of KA (100 nM) and CCh (5 μM). We first tested for involvement of GABAergic mechanisms. Application of the $GABA_A$ receptor antagonist gabazine (250 nM) reduced modal peak beta oscillatory power to 49.0 ± 8.2% of baseline and cumulative application of gabazine to 2 μM further reduced beta power to 32.4 ± 4.6% of baseline ($P < 0.001$ in both cases, n = 10, see Fig. 1B). Further involvement of GABAergic mechanisms was confirmed by application of the GABA uptake blocker, tiagabine (1 μM) (Fig. 1C), which enhanced modal peak oscillatory power (180.7 ± 24.7% of control, <0.05, n = 6). Interestingly, a higher concentration of tiagabine (10 μM) depressed modal peak power (80.2 ± 25.4% of control, $P < 0.01$, n = 6).

To investigate the role of the benzodiazepine site in modulation of beta oscillations, we tested the effects of the benzodiazepine-site agonist, zolpidem. In previous *in vitro* studies, zolpidem has often been used at μM concentrations (e.g. Pálhalmi et al., 2004; Koniaris et al., 2011). We have reported that zolpidem depresses neuronal oscillatory activity *in vivo* in the cortex of stroke (Hall et al., 2010) and Parkinson's disease (Hall et al., 2014) patients at sub-sedative doses (5 mg). Plasma concentration after oral administration of 5–10 mg of zolpidem is in the range of 14–93 ng/mL (Olubodun et al., 2003; Greenblatt et al., 2006). Zolpidem is approximately 92% bound by plasma proteins (Salvà and Costa, 1995), suggesting that the effective concentration of zolpidem *in vivo* may be in the nM range; hence we chose to explore the effects of low nanomolar concentrations of zolpidem *in vitro*.

Consistent with our observations *in vivo*, zolpidem at 10 nM robustly depressed modal peak beta power (to 60.2 ± 6.8% of control, $P < 0.001$, n = 21; Fig. 2).

It is generally accepted that benzodiazepine site agonism causes an enhancement of beta activity or 'beta buzz' (Glaze, 1990), so we explored the dose-dependency of benzodiazepine-site modulation by constructing cumulative dose response curves (30–500 nM). In contrast to the depression of beta power with 10 nM zolpidem, an enhancement was seen at 30 nM (319.2 ± 119.9%, $P < 0.05$, n = 7; Fig. 3). We repeatedly attempted to construct concentration–response curves for the complete range of concentrations from 10 to 500 nM. However, we found that once oscillatory power

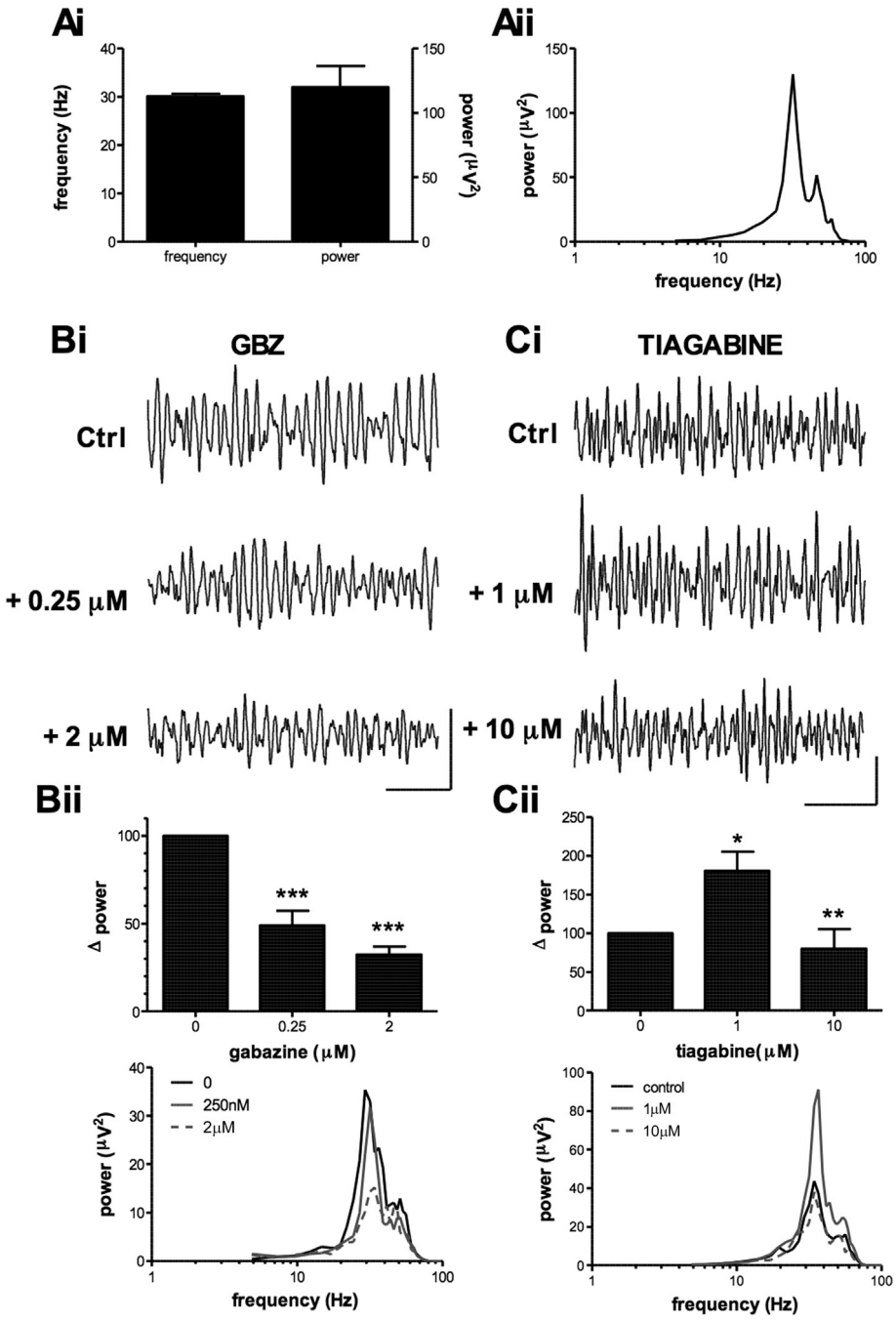

Fig. 1. Beta oscillations in M1 are dependent on GABAergic inhibition. Ai) Mean frequency and power of beta oscillations in M1. Aii) Representative power spectrum of beta activity in M1 *in vitro*. Bi) Raw data traces showing typical effects of gabazine (250 nM and 2 μM) on oscillatory activity in M1. Bii) Pooled data showing change in peak beta power in the presence of gabazine and representative power spectra. Ci) Raw data traces showing typical effects of tiagabine (1 μM and 10 μM) on oscillatory activity in M1. Cii) Pooled data showing change in peak beta power in the presence of tiagabine and representative power spectra. Scale bars 200 ms × 50 μV. $^{*}P < 0.05$, $^{**}P < 0.01$, $^{***}P < 0.001$.

had been depressed by 10 nM zolpidem it was not possible to augment oscillatory power with higher concentrations.

Zolpidem clearly had two discernible effects, with reduction of oscillatory power at 10 nM and clear augmentation at 30 nM. At higher concentrations (100–500 nM), the drug began to depress beta power again, but this effect was quite variable, so we focused further experiments on the repeatable effects of zolpidem at 10 and 30 nM.

In view of the narrow concentration threshold between inhibition and augmentation of oscillatory activity, we examined the benzodiazepine-site specificity of the different effects of zolpidem, by repeating the previous experiments in the presence of a benzodiazepine-site antagonist. Flumazenil (500 nM), prevented both the depressing and potentiating effects of zolpidem (Fig. 4Ai and Aii). This indicates that zolpidem exerts both effects on beta power through the benzodiazepine binding site. Interestingly, application of flumazenil alone significantly augmented oscillatory power (276.7 ± 111.4% of control at 100 nM, 292.1 ± 90.8% at 200 nM and 273.2 ± 90.0% at 500 nM, n = 6, $P < 0.05$, Fig. 4Bi and Bii).

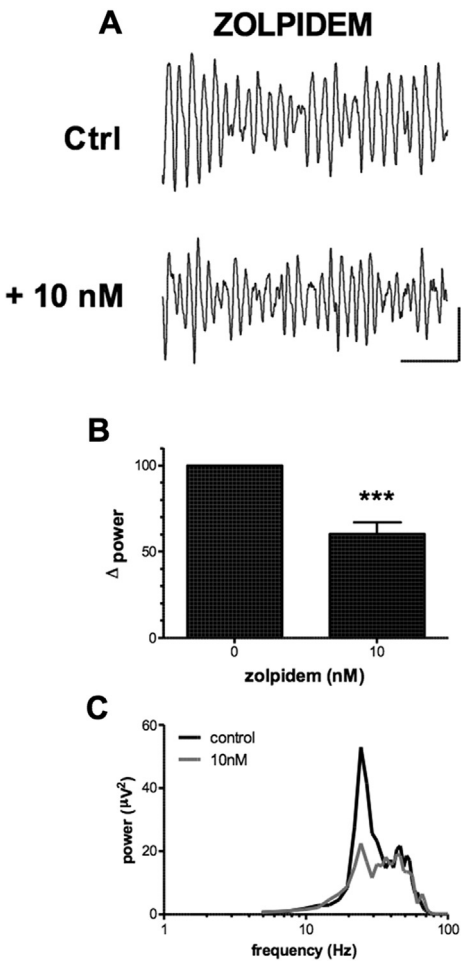

Fig. 2. 10 nM zolpidem reduces beta oscillatory power. A) Raw data traces showing the reduction in oscillatory activity induced by bath application of zolpidem at 10 nM. B) Bar charts of pooled data showing a reduction in beta oscillatory power induced by zolpidem (10 nM). C) Representative power spectra. Scale bars 200 ms × 50 μV. $^{***}P < 0.001$.

3.2. Effects of benzodiazepine binding on phasic and tonic $GABA_AR$ currents

We have recently reported a depression of pathological theta/beta oscillations associated with alleviation of stroke related deficits in cognitive function (Hall et al., 2010), by sub-sedative doses of zolpidem in a stroke patient. Similarly, we have described benefits of low-dose zolpidem treatment in patients with Parkinson's disease (Hall et al., 2014). Thus, the inhibition of beta activity by zolpidem at a low concentration (10 nM) was of particular interest. Zolpidem could alter phasic and/or tonic inhibition GABAergic inhibition (Nusser and Mody, 2002; Semyanov et al., 2003; Gao and Smith, 2010), so we investigated these possibilities in pyramidal and FS interneurons in M1.

3.2.1. Tonic and phasic inhibition in pyramidal cells

We made whole-cell voltage clamp experiments from pyramidal neurons in layer V. To establish whether the effects of zolpidem we saw in LFP recordings of network activity were related to GABAergic neuronal activity we recorded sIPSCs, which reflect inhibitory activity from local networks of GABAergic neurons. Fig. 5 shows that application of KA and CCh elicited rhythmic sIPSCs at beta (and lower) frequency, evidenced as a peak at 15–20 Hz in the fast Fourier transform of the data. Addition of zolpidem (Fig. 5B) significantly depressed peak beta power, ($P < 0.05$; n = 6; Fig. 5C). Mean area power (between 13 and 29 Hz) was 64.7 ± 27.9 pA s, increasing to 521.4 ± 302.1 pA s in KA and CCh and decreasing to 327.9 ± 86.1 pA s in zolpidem. Although beta frequency in submerged recording conditions was lower than that seen in interface LFP recordings, it was clear that zolpidem had a similar effect at low concentrations, and that these effects were related to rhythmic inhibitory activity generated by GABAergic neurons impinging on principal cells.

A change in rhythmic sIPSCs could be attributable to a direct reduction in presynaptic release of GABA, inhibition of postsynaptic receptors, or indirect reduction of GABA release via depression of interneuronal excitability, and might be mediated via phasic or tonic inhibition on principal cells or interneurons. We explored these possibilities using zolpidem at concentrations found to either depress or augment beta oscillatory power.

In voltage clamp recordings from pyramidal cells, a tonic current (mean 14.7 ± 4.8 pA, n = 13) was revealed by blockade of $GABA_A$ receptors with bicuculline (20 μM). Zolpidem (10 nM) had no significant effect on I_{tonic} (2.4 ± 6.6 pA, $P > 0.05$, n = 6). Zolpidem also failed to modulate I_{tonic} at 30 nM (mean change 2.3 ± 7.4 pA, $P > 0.05$, n = 7). These data suggested that pyramidal cell I_{tonic} was zolpidem-insensitive. We also examined the kinetics of sIPSCs recorded in pyramidal neurons during application of 10 and 30 nM zolpidem, and found no significant change in mean-median IEI, amplitude or decay time constant, indicating that phasic inhibition in pyramidal cells is also unaffected by zolpidem at the concentrations used (See Supplementary figures for analyses of tonic and phasic currents in pyramidal cells).

3.2.2. Phasic inhibition in FS cells

In order to address similar questions in FS cells, Betz cells in layer V were first located on the basis of size, orientation and morphology, and FS cells then identified through their own characteristic morphology and location adjacent to Betz cells (Fig. 6A). The stereotypical arrangement between Betz and GABAergic interneurons was confirmed, as previously reported (Ali et al., 2001; Ali, 2003). In FS cells (n = 6) depolarizing current injection, elicited high frequency (80–198 Hz) non-adapting spikes with short duration at half amplitude (0.76 ± 0.03 ms), a pronounced medium after-hyperpolarization (AHP; 17.4 ± 1.6 mV) with no slow AHP, and a mean input resistance of 99.0 ± 6.0 MΩ (Fig. 6B). There was no evidence of a depolarizing sag in the response to hyperpolarizing current injection. These characteristics are similar to those described previously for FS cells in M1 (Kawaguchi, 1995; Cauli et al., 1997; Kawaguchi and Kubota, 1997; Ali et al., 2001). In subsequent studies we used voltage-clamp recording to assess phasic and tonic GABAergic inhibitory currents in FS neurons.

We showed above that gabazine (250 nM) inhibited beta oscillations in LFP recordings. In FS neurons, gabazine markedly reduced sIPSC amplitude from 18.7 ± 5.0 pA to 11.8 ± 2.0 pA ($P < 0.05$; n = 6) and mean IPSC decay time was reduced from 6.1 ± 1.0 to 4.4 ± 1.0 ms ($P < 0.05$). A tendency towards increased IEI (201 ± 72 ms v 380 ± 214 ms) did not reach significance (see Supplementary figures).

We found that low concentrations of zolpidem had no discernible effect on sIPSCs Thus; zolpidem (10 nM) had no effect on the distribution of IEI (mean 343.9 ± 124.4 ms v 250.0 ± 75.5 ms; $P > 0.05$, KS) or amplitude of sIPSCs (mean 47.7 ± 4.2 pA v 48.0 ± 2.1 pA; $P > 0.05$, KS) in FS neurons (n = 6). Decay time (10–90%) was also unaffected (6.7 ± 1.1 ms v 6.2 ± 0.83 ms; $P > 0.05$). Similar observations were made with 30 nM zolpidem (see Supplementary figures).

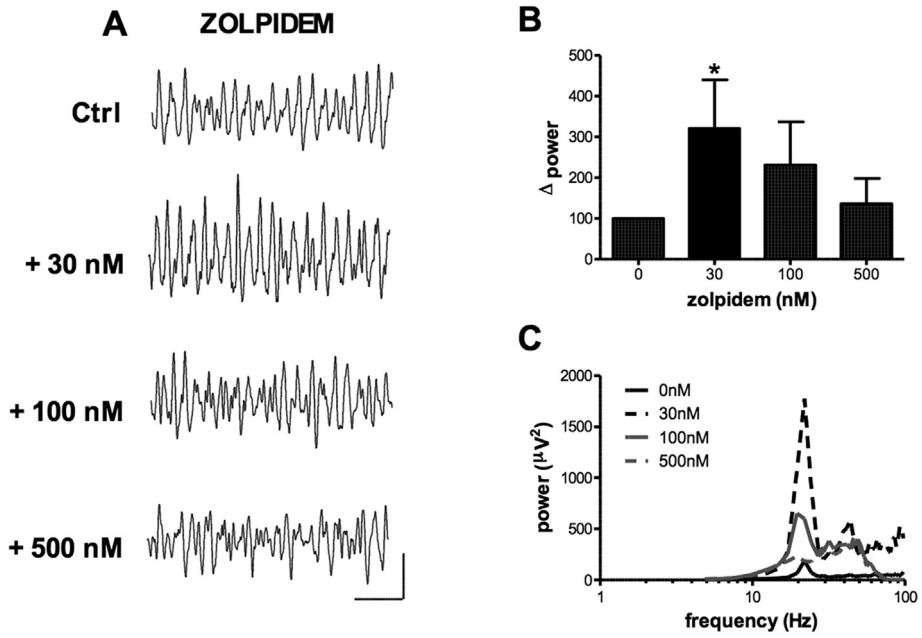

Fig. 3. Concentration-dependent modulation of oscillatory power by zolpidem. A) Raw data traces showing the effect of different doses of zolpidem (30–500 nM) on beta oscillatory activity. B) Bar chart of pooled data showing a reduction in beta oscillatory power induced by zolpidem (30–500 nM). C) Representative power spectra. Scale bars 200 ms × 50 μV. $^{*}P < 0.05$.

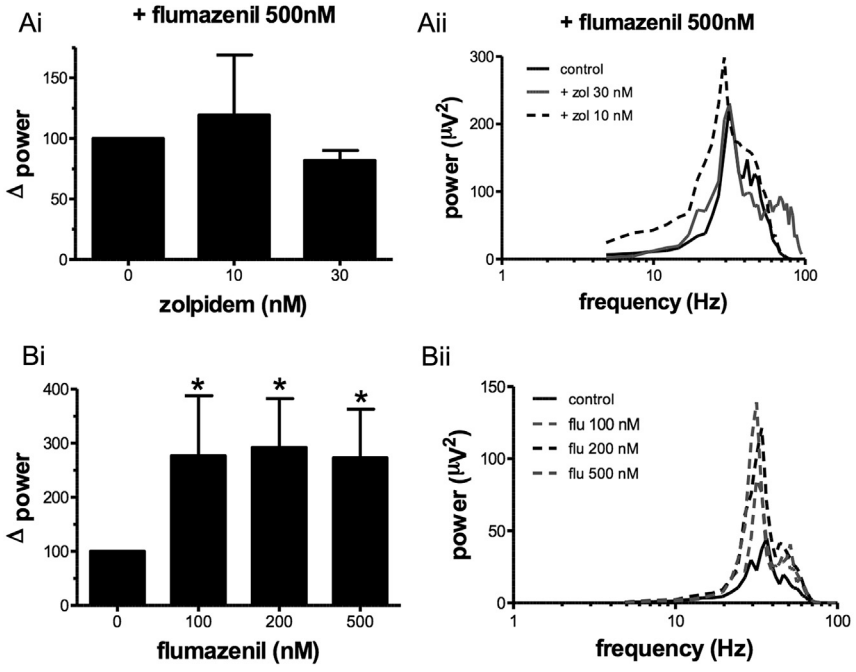

Fig. 4. Flumazenil (500 nM) blocks zolpidem induced depression and augmentation of beta power. Ai) Pooled data showing flumazenil blockade of the effects of zolpidem at 10 and 30 nM on modal peak beta oscillatory power. Aii) Power spectra of typical data recorded during flumazenil blockade of zolpidem responses. Bi) Bar chart showing effects of increasing concentration of flumazenil on beta power. Bii) Representative power spectrum showing increase in oscillatory power obtained in flumazenil (100–500 nM). Scale bars 200 ms × 50 μV. $^{*}P < 0.05$.

3.2.3. *Effects of 10 nM zolpidem on I_{tonic} in FS cells*

Given that we could find no effect of 10 nM zolpidem on phasic inhibition impinging on GABAergic neurons in M1, we analysed the effects of zolpidem application on tonic inhibition. Since tonic inhibition has not previously been demonstrated in FS cells in M1, we first tested the effects of the competitive $GABA_A$ receptor antagonist, gabazine (250 nM). As Fig. 6C shows, gabazine revealed a tonic current (mean 10.3 ± 4.4 pA, $P < 0.05$ compared to baseline fluctuation; n = 5). Subsequent co-application of bicuculline (20 μM) removed the small residual current, although overall there was no significant change compared to gabazine alone (2.5 ± 2.3 pA). Application of bicuculline alone (20 μM), as Fig. 6D shows, also caused a decrease in holding current (22.66 ± 3.55 pA, n = 6, $P < 0.001$). These data indicated that a tonic current was indeed

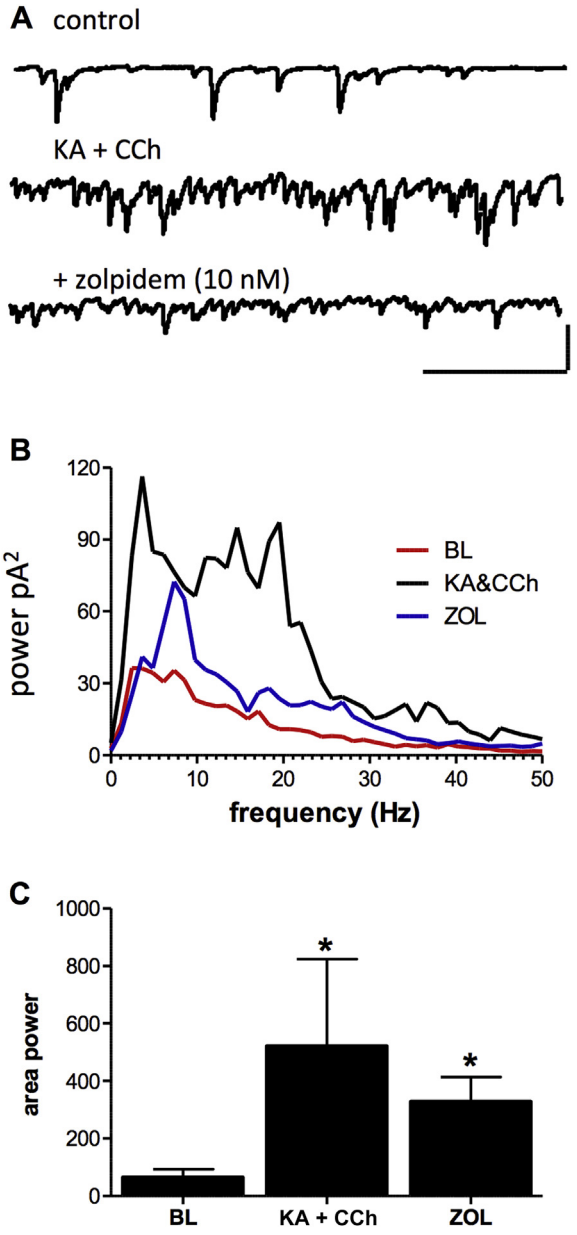

Fig. 5. Zolpidem reduces rhythmic IPSC activity in FS cells. A) Raw traces showing the effects of zolpidem on KA + CCh induced sIPSC activity in an FS cell. Scale bars 500 ms × 200 pA. B) Power spectrum (30 data segments) from the recording in A), showing effects of zolpidem on spectral power. C) Pooled data showing effects of zolpidem (10 nM) on area power at 15–29 Hz. *$P < 0.05$.

present in inhibitory neurons in M1. We next assessed the sensitivity of I_{tonic} to zolpidem. At 10 nM, zolpidem itself generated a slow, inward current (mean amplitude 15.0 ± 3.5 pA; n = 6; Fig. 7A,D). Subsequent application of bicuculline (20 μM) abolished I_{tonic} suggesting that the increase in inward current by zolpidem was due to augmentation of existing I_{tonic}. Indeed, bicuculline always reduced I_{tonic} beyond the pre-zolpidem baseline, showing the presence of a non-zolpidem induced component of tonic current in the inhibitory neurons. To determine whether two components could be differentiated, we attempted to modulate I_{tonic} through alteration of ambient GABA concentration. We pre-applied GABA (1 μM), which induced in a large inward current (70.0 ± 14.1 pA; n = 6, $P < 0.05$; Fig. 7B,D). Subsequent addition of zolpidem (10 nM) generated a further inward current, of the same magnitude as that

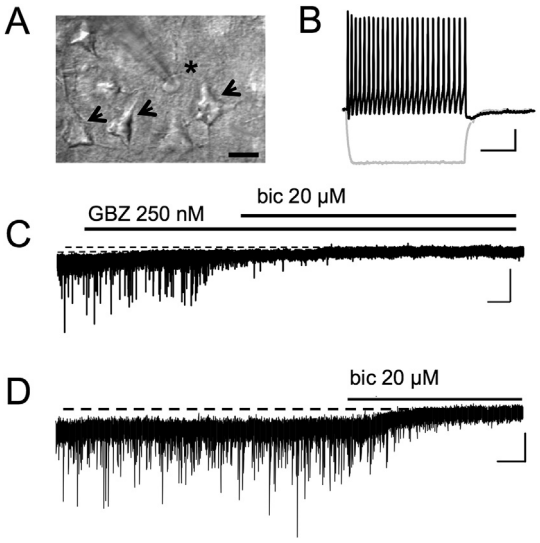

Fig. 6. Identification of FS interneurons. A) Photo-micrograph showing recording electrode and putative FS interneuron (asterisk) in close proximity to Betz cells (arrows) in LV of M1. Scale bar 25 μm. B) Voltage traces of the FS cell identified in A), in response to −400 pA and +100 pA current steps. Scale bars 25 mV, 50 ms. Note the high firing frequency (>100 Hz) and action potentials with large AHPs. C) Representative voltage-clamp recording from a FS interneuron at a holding potential of −70 mV during application of gabazine (250 nM) and bicuculline (20 μM). Scale bar 100 pA, 2 min. D) Representative voltage-clamp recording from a FS interneuron at a holding potential of −70 mV during application of bicuculline alone. Scale bar 100 pA, 2 min.

seen without addition of GABA (14.9 ± 5.1 pA; $P < 0.05$; Fig. 7B,D), suggesting that at 10 nM, the I_{tonic} induced by zolpidem did not depend on ambient GABA concentration.

Previous reports have indicated that I_{tonic} is often linked to the presence of the delta (δ) subunit within extrasynaptic GABA receptor complexes (Nusser et al., 1998) so we studied the subunit composition of receptors mediating I_{tonic} in FS cells using the δ-subunit-selective agonist, THIP. THIP has been reported to be selective for δ-subunit containing receptors at up to 800 nM (Meera et al., 2011), so we used a slightly higher concentration of THIP (1 μM) look for occlusion of the zolpidem mediated augmentation of I_{tonic}. THIP alone had no effect on phasic inhibition (data not shown) but did induce a slow inward current in FS cells (Fig. 7C,D). After stabilization of the THIP-induced current (mean 17.1 ± 11.6 pA; n = 6), a further increase in I_{tonic} was induced by co-application of zolpidem at 10 nM (14.9 ± 6.7 pA), and the difference was significant (Fig. 7C,D; $P < 0.05$). These data suggest that a pool of THIP-sensitive, δ-subunit containing receptors mediates a component of I_{tonic} in FS cells, but that these receptors are not the same as those mediating the effects of zolpidem.

Finally, it should be noted that when bicuculline (20 μM) was applied prior to zolpidem, both phasic and tonic inhibition were abolished, and changes in holding current in response to zolpidem were not seen (n = 6, data not shown), indicating that both forms of I_{tonic} were mediated by bicuculline-sensitive $GABA_A$ receptors.

3.3. *Effects of benzodiazepine site antagonism on tonic and phasic inhibition in FS cells*

We further examined the role of the benzodiazepine site on the effects of zolpidem using the antagonist flumazenil. Flumazenil (500 nM) had no effect on phasic inhibition (Fig. 8A,B). The mean IEI of sIPSCs in control was 416.5 ± 14.7 ms compared to 488.5 ± 19.6 ms in flumazenil (n = 6; $P > 0.05$ KS), and sIPSC amplitude was also unaltered (81.8 ± 1.4 pA v 80.0 ± 1.4 pA; $P > 0.05$ KS).

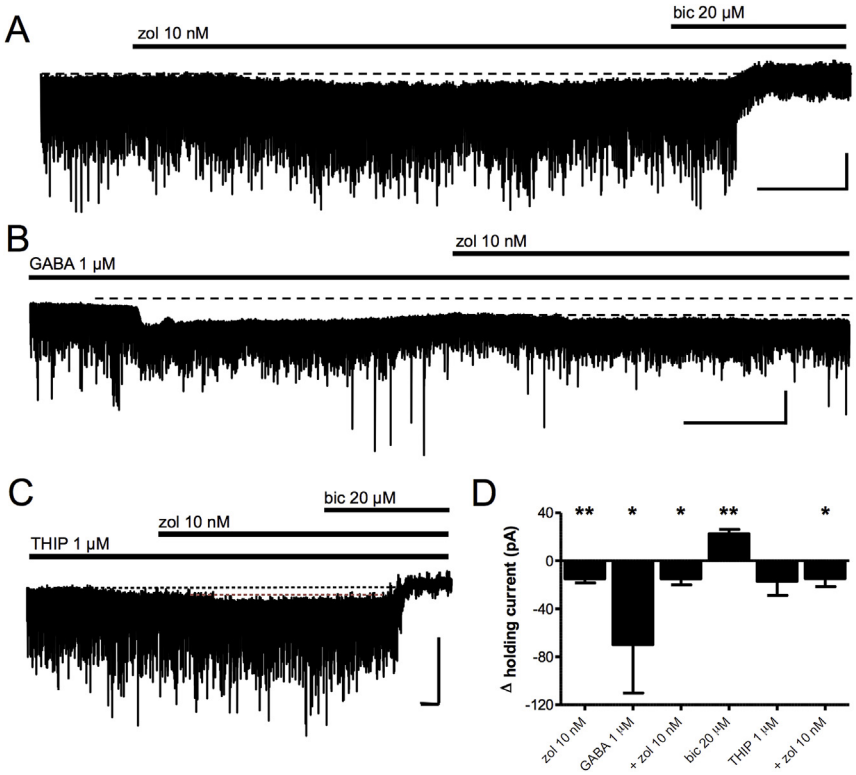

Fig. 7. Zolpidem (10 nM) augments a tonic inhibitory current in FS interneurons. A) Representative recording showing zolpidem (10 nM) induction of I_{tonic}. Subsequent addition of bicuculline (20 μM) abolished both phasic IPSCs and zolpidem-induced tonic current. Scale bar 50 pA, 2 min. B) Representative recording showing a GABA and zolpidem induced tonic current. Note that the GABA current is desensitizing, but the zolpidem current is not. Scale bars 100 pA, 5 min. C) Voltage-clamp recording from an FS interneuron at a holding potential of −70 mV. Addition of THIP (1 μM) induced a tonic current. Subsequent addition of zolpidem (10 nM) augmented the current and the effect of both drugs was blocked by bicuculline (20 μM). Scale bar 100 pA, 2 min D) Histogram showing mean change in holding current induced by zolpidem (10 nM), GABA (1 μM), GABA (1 μM) + zolpidem (10 nM), bicuculline (20 μM) alone, THIP and further changes induced by co-addition of zolpidem. $^{*}P < 0.05$, $^{**}P < 0.01$.

However, when applied alone, flumazenil decreased the holding current (31.3 ± 13.9 pA; $P < 0.01$, n = 6), demonstrating that I_{tonic} in FS cells depends on benzodiazepine-site activity. If the inhibitory effects of zolpidem on beta oscillations were mediated via the zolpidem-sensitive tonic current in FS cells, then we may expect the zolpidem (10 nM) induced augmentation of I_{tonic} to be blocked by flumazenil. This was indeed the case, as when zolpidem (10 nM) was applied in the presence of flumazenil no further change in holding current was observed (Fig. 8C).

3.4. Effects of 30 nM zolpidem on phasic and tonic inhibition in FS cells

As described above, 30 nM zolpidem elicited an increase in oscillatory power, suggesting that the higher concentration may have an additional effect on phasic inhibition, and/or a different effect on I_{tonic}, so we explored the effects of zolpidem at 30 nM on phasic and tonic inhibition in FS cells. Zolpidem at 30 nM, as at 10 nM, had no effect on IEI, amplitude or decay time of sIPSCs (data not shown). However, in contrast to its effects at 10 nM where it augmented I_{tonic}, at 30 nM zolpidem elicited a *decrease* in I_{tonic} (17.8 ± 20.4 pA; $P < 0.05$; n = 6; Fig. 9A,C).

3.5. The role of desensitization in the differential effects of zolpidem in FS cells

Since the effects of benzodiazepine site ligands might be expected to differ depending on receptor occupancy, and since both occupancy and benzodiazepine binding might alter $GABA_A$ receptor dynamics such as desensitization and resensitization, we recorded I_{tonic} under conditions in which GABA concentration was fixed at a sub-saturating level of 1 μM. At 1 μM (Fig. 9B,C), GABA induced a maximum inward current (78.62 ± 47.5; $P < 0.05$; n = 6) and steady state desensitization (28.3 ± 7.6; $P < 0.05$). In contrast to its effects at ambient GABA levels, application of 30 nM zolpidem in the presence of 1 μM GABA, elicited an *increase* in I_{tonic} (82.3 ± 37.6 pA; $P < 0.05$; n = 6; Fig. 9B,C) and this was followed by rapid desensitization of the zolpidem-induced response (28.3 ± 7.6 pA). The large increase in tonic current and the desensitization profile observed in the presence of 1 μM GABA suggested that a robust desensitization process was taking place.

Using the kinetic simulation model described in the methods we have simulated the experimental data described above. The model contains the presence of open and desensitized states for the unbound receptor and clearly shows the opposing effects of low and higher dose zolpidem. Fig. 10 shows the Markov models for GABA (Fig. 10A) and zolpidem (Fig. 10B) binding; the rate constants used (Fig. 10C) were first estimated using the parameters of Jones and Westbrook (1995).

As Fig. 7A showed, zolpidem at 10 nM caused an increased I_{tonic}. In the kinetic model, this behaviour was also seen (Fig. 10Di). By contrast, zolpidem caused a decrease in I_{tonic} at 30 nM (Fig. 9A), and again this was captured in the behaviour of the model (Fig. 10Dii), with the distribution of receptor-ligand states suggesting that this is related to enhanced entry into rapidly desensitized states. When we 'applied' zolpidem in the presence of 1 μM GABA in the model (Fig. 10Diii), 30 nM zolpidem caused a clear (and relatively large) increase in I_{tonic} followed by a clear desensitization, analogous to the situation shown in Fig. 9B.

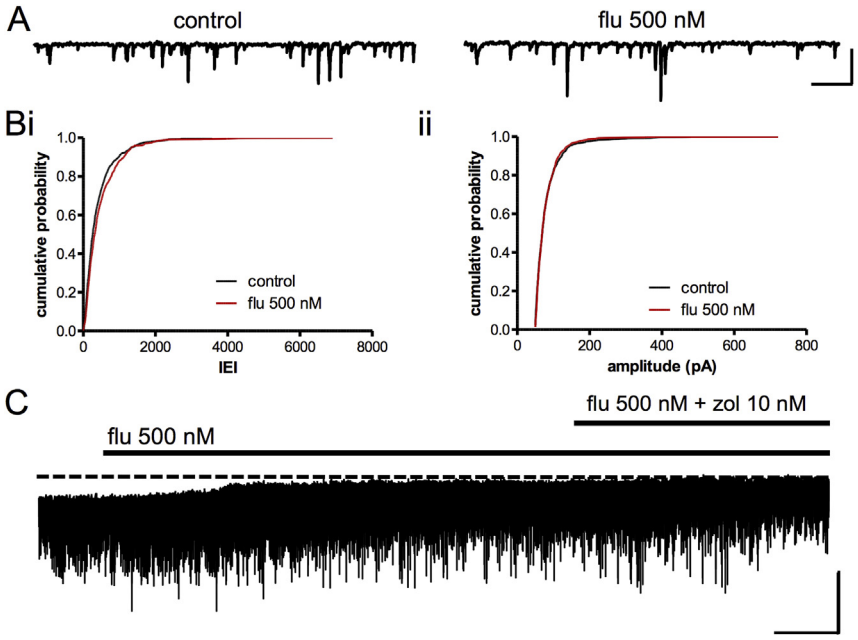

Fig. 8. Flumazenil (500 nM) reduces the tonic inhibitory activity and blocks the zolpidem-induced tonic current in FS interneurons. A) Representative traces from single experiment showing sIPSCs in control and flumazenil (500 nM). Scale bars 50 pA × 500 ms. Bi) Cumulative probability plot showing there was no significant change in the frequency of sIPSCs with the addition of flumazenil (500 nM). Bii) Cumulative probability plot showing there was no significant difference to sIPSC amplitude with the addition of flumazenil (500 nM). C) Representative voltage-clamp recording from a FS interneuron at a holding potential of −70 mV. Addition of flumazenil (500 nM) slowly reduced a tonic current. Subsequent addition of zolpidem (10 nM) was without effect. Scale bars 100 pA, 5 min.

Both experiment and the model indicated that at a concentration of 10 nM, zolpidem induces a consistent, low amplitude I_{tonic} that is independent of ambient GABA concentration. By contrast, at 30 nM, zolpidem induces changes in I_{tonic} whose magnitude and even direction is highly dependent on ambient GABA. We interpreted these data to indicate that at 10 nM, zolpidem falls below the threshold for exerting effects on GABA receptor affinity, instead working to enhance channel opening through effects on gating in a subpopulation of GABA receptors. At 30 nM, zolpidem begins to affect the GABA unbinding rate, and this is manifest as a greatly enhanced I_{tonic} in the presence of 1 μM GABA, which was as large as the current induced by 1 μM GABA itself. These affinity effects are also manifest as rapid desensitization events, seen clearly at 30 nM in the presence or absence of applied GABA.

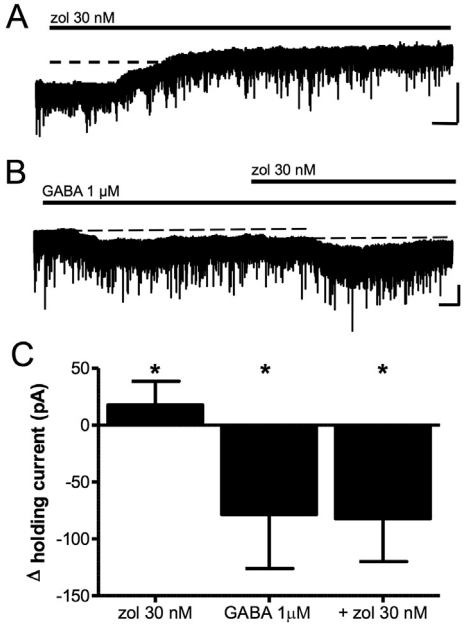

Fig. 9. Zolpidem (30 nM) inhibits tonic current without effect on phasic IPSCs in FS interneurons. A) Voltage-clamp recording from an FS interneuron at a holding potential of −70 mV. Addition of zolpidem (30 nM) reduced a tonic current. Scale bar 100 pA, 5 min. B) Voltage-clamp recording from an FS interneuron. Addition of GABA (1 μM) induced a large inward current, which was increased by further addition of zolpidem (30 nM). Note the desensitization of the tonic current that takes place in both GABA and zolpidem. Scale bar 100 pA, 1 min. C) Bar chart showing change in holding current induced by the addition of zolpidem (30 nM), GABA (1 μM) and GABA (1 μM) + zolpidem (30 nM). $^*P < 0.05$.

The experiments with 30 nM zolpidem indicated that at different concentrations of zolpidem and ambient GABA, we were observing differences in the rate and extent of steady state desensitization of GABA receptors on FS cells. Entry into and out of desensitized states is controlled, at least in part, through the degree of binding of the GABA receptor. For example, at synaptic levels of GABA, desensitization is rapid, and exit and entry to and from open and desensitized states play a major role in shaping the decay phase of the GABA IPSC. At lower levels of GABA, however, receptor occupation is unlikely to be high, and channel kinetics are altered. Recently, an elegant study of receptors modified to disable dual binding (Petrini et al., 2011) reported that mono-liganded GABA receptors showed dramatically slowed kinetics compared to dual bound receptors, and that entry and exit from desensitization was particularly slow at very low levels of receptor occupancy. We hypothesized that, in the presence of nanomolar ambient GABA and 10 nM zolpidem, receptor binding would be low and effects of zolpidem on K_{off} would be negligible, such that slow entry and exit from a desensitized state similar to that described by Petrini et al. (2011) would be favoured. By contrast, this would not be so at 30–1000 nM, when effects on K_{off} dominate, and when zolpidem induced rapid desensitization would be readily observed (as in Fig. 9B) and may even be enhanced by benzodiazepine binding (Mellor and Randall, 1997). Benzodiazepine site mediated effects on K_{off} cannot affect the maximal rate and extent of responses to saturating concentrations of GABA (Bianchi et al., 2009;

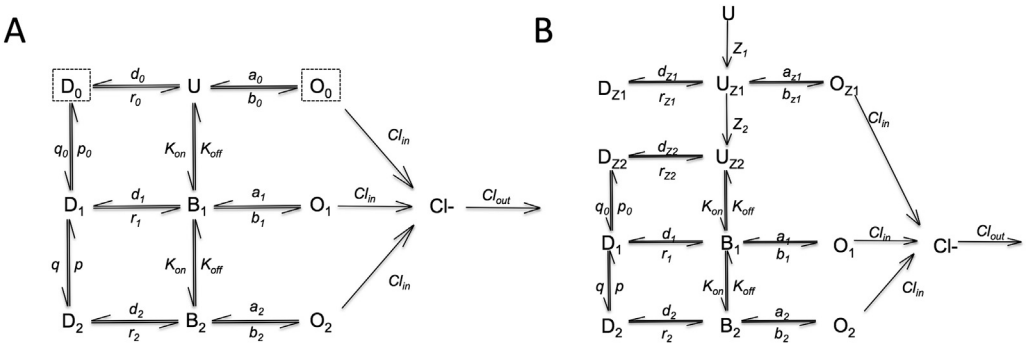

C

Rate Constant [a]	GABA model	Zolpidem model [b] High affinity	Zolpidem model [b] Low affinity
k_{on}	5 x10^{b}	-	+
k_{off}	600	-	300
z_1	-	5 x10^{8}	-
z_2	-	-	5 x10^{6}
b_1	2227^{b}	-	+
a_1	104.5^{b}	-	45
b_2	3074^{b}	-	+
a_2	116.6^{b}	-	75
d_1	13	-	+
r_1	0.2	-	+
d_2	1000	-	+
r_2	30	-	+
p	1	-	+
q	0.01	-	+
b_0	0.215^{b}	75	-
a_0	53.5^{b}	+	-
d_0	0.001^{b}	1.5	0.002
r_0	0.09^{b}	0.1	0.1
p_0	0.14^{b}	-	+
q_0	0.37^{b}	-	+
Cl_{in}	4000	+	+
Cl_{out}	200	+	+

[a] Rate constant units $M^{-1}s^{-1}$ for ligand binding rates k_{on}, k_{off}, z_1, z_2, Cl_{in} and Cl_{out}. All others are s^{-1}. [b] Rates were first estimated using the parameters from Jones and Westbrook (1995) and then optimised to fit data generated in Figure 6B. Rates shared across models indicated by + and unused parameters denoted as –.

Fig. 10. Simulation of experimental data. A) Markov model containing unbound state (U) and two transition states (B_1 and B_2), two open states (O_1 and O_2) and two desensitized states (D_1 and D_2) both of which occur following GABA binding. Further to this, we have proposed the existence of an additional open (O_0) and desensitized state (D_0) both occurring from the unbound state (dashed boxes in scheme). B) Model accounting for zolpidem binding depicted this as a two-state binding event. The first is a higher affinity state (UZ1) and the second, a lower affinity state (UZ2). O and D refer to open and desensitized states, respectively. C) Rate constant table for the schemes in A and B. Di) Simulation of experimental data in Fig. 3B (10 nM zolpidem). Dii) Simulation of experimental data in Fig. 5A (30 nM zolpidem). Diii) Simulation of experimental data in Fig. 5B (30 nM zolpidem in 1 μM GABA).

Bianchi, 2010). However, if, at 10 nM, zolpidem was mediating effects on GABA receptors primarily through effects on mono- or unliganded, kinetically slow entry and exit from desensitized states, this would be revealed as a submaximal response to challenge with saturating GABA.

We therefore tested for a population of kinetically slow desensitized $GABA_A$ receptors by pre-incubating in 10 nM, 30 nM or 1 μM zolpidem and subsequently challenging with saturating (1 mM) GABA in the continued presence of zolpidem. Application of 1 mM GABA alone typically elicited a large inward current (976.9 ± 184.1 pA, n = 8), followed by desensitization (τ 19.74 ± 1.37 s, extent 366.4 ± 96.50 pA, n = 8), to a steady-state (478.7 ± 197.3 pA, n = 8). We then measured the maximal and steady-state current, and the rate and extent of desensitization in a series of experiments in which GABA (1 mM) was applied after pre-incubation (for 60 min) in different concentrations of zolpidem. Zolpidem was also present in the bath at the pre-incubation level for the duration of the experiment. As Fig. 11 shows, at both 30 nM and 1 μM, the effects of saturating GABA were not significantly different to control (n = 6 in each group), with large maximal current, rate and extent of desensitization and steady-state values. Indeed, discernible changes to the desensitization parameters were only visible after pre-incubation with 10 nM zolpidem. Here, the application of GABA resulted in much reduced maximal and steady-state currents and a lesser rate

and extent of desensitization compared to GABA alone, (Fig. 11Ai&B, 10 nM zolpidem; maximum current 448.7 ± 54.93 pA, τ 71.19 ± 21.43 s, extent 127.3 ± 29.99 pA, steady-state 142.3 ± 26.56 pA, $P < 0.05$, $n = 6$). Summary data are presented in Fig. 11B). These data strongly suggest that a population of receptors was sequestered into a kinetically slow desensitized state by incubation with 10 nM zolpidem and that such receptors were then unavailable to participate in further desensitization processes. We tested this hypothesis using an *in silico* approach, applying a 'saturating concentration' of GABA in a model that allowed analysis of the individual receptor species concentrations after pre-incubation with different 'zolpidem concentrations'.

When we repeated the experiments *in silico*, the model showed a profile consistent with the *in vitro* data, such that GABA induced a large peak and desensitization to a steady-state. Hence, control, 30 nM and 1 μM zolpidem simulations showed extensive desensitization, with large 'currents' and rapid kinetics. In excellent agreement with the *in vitro* experiments, 10 nM zolpidem occluded these effects to a significant degree (Fig. 11Aii). The model predicted a reduction in the population of receptors immediately available for maximal activation and desensitization in response to 1 mM GABA. Analysis of the individual receptor species concentrations revealed that after incubation with 10 nM zolpidem, 54.9% of GABA receptors were unavailable for binding in 1 mM GABA, compared to only 12.1% of receptors following incubation in 1000 nM zolpidem. Hence, the kinetically slow desensitization produced by 10 nM zolpidem incubation appeared to have prevented GABA binding during the challenge with saturating GABA, whilst higher concentrations of zolpidem favoured kinetically rapid transitions between states and allowed ≈90% of receptors to bind GABA and become rapidly desensitized.

4. Discussion

4.1 Beta oscillations and FS interneurons in M1

FS cells preferentially form synaptic connections at perisomatic and proximal dendritic regions of numerous neighbouring pyramidal cells, and are thus able to exert powerful control over large assemblies of neurons (Cobb et al., 1995). The characteristic features of FS cells, which include short duration action potentials, high frequency firing with no adaptation, reliable synchronous GABA release and rapidly decaying IPSPs onto principal cells, mediated by receptors containing the α1 subunit (Thomson et al., 2000), appear crucial for both coherence of network oscillations and frequency control (Bartos et al., 2001, 2002). Recently, Manseau et al. (2010) have reported the asynchronous release of GABA at autaptic and synaptic contacts from FS interneurons, highlighting the fact that these cells control both synchronization and desynchronization processes in cortical networks and underlying their pivotal position in network function.

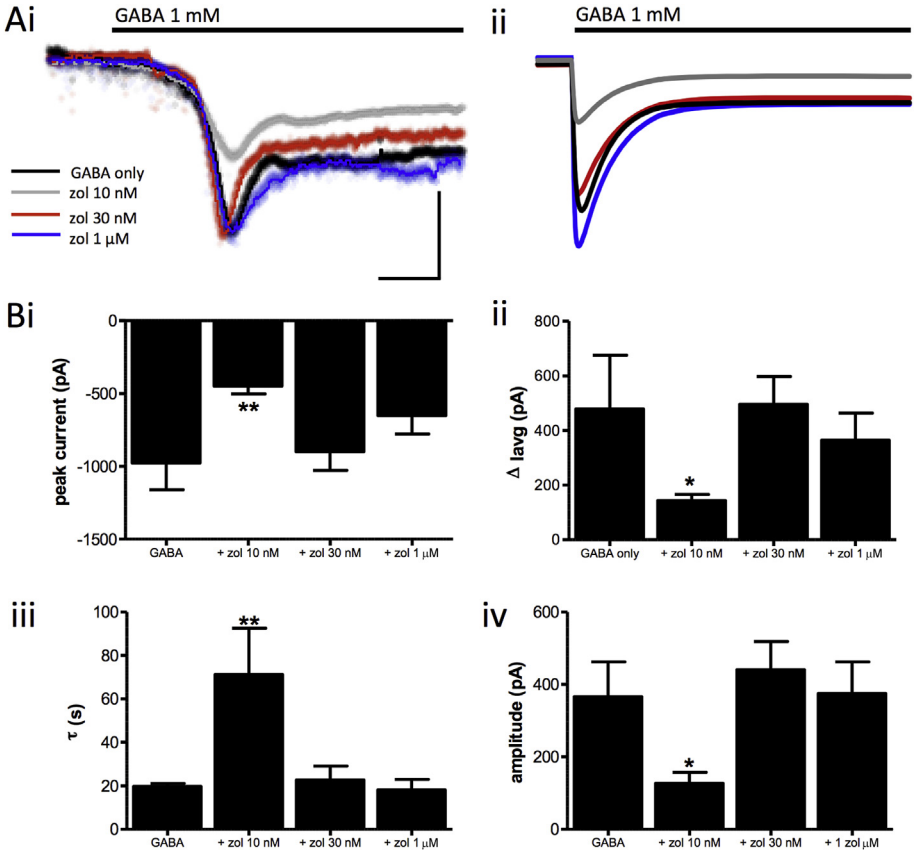

Fig. 11. Zolpidem (10 nM) blocks fast desensitization processes in FS interneurons. Ai) Voltage-clamp traces showing pre-incubation of slices in 10 nM (grey), 30 nM (red) and 1 μM zolpidem (blue) have differing effects on desensitization processes. Aii) Simulation of experimental data in Bi. Bi) Bar chart showing maximum current induced by addition of 1 mM GABA after pre-incubation with zolpidem (10, 30, 1000 nM). Bii) The steady state response is reduced after pre-incubation with zolpidem (10 nM). Biii) The decay time constant of desensitization is significantly increased and Biv) the amplitude of desensitization is significantly reduced after pre-incubation with zolpidem (10 nM). $^{*}P < 0.05$, $^{**}P < 0.01$. (For interpretation of the references to colour in this figure legend, the reader is referred to the web version of this article.)

4.2 FS interneurons and I_{tonic}

In addition to phasic synaptic inhibition, CNS neurons are also subject to persistent, tonic inhibition. Due to the substantial charge transfer associated with tonic inhibition, its effects are profound and include altering excitability of individual neurons as well as influences on excitatory synaptic efficacy and integration (Farrant and Nusser, 2005). It has been demonstrated that differential regulation of GABA uptake (Semyanov et al., 2003) enhances I_{tonic} FS cells compared to that seen in pyramidal cells. Hence, I_{tonic} in FS cells appears likely to exert powerful control over network activity, and, indeed, eliminating tonic inhibition in interneurons has been shown to increase the power of gamma activity in CA1/CA3 of the hippocampus (Mann and Mody, 2010).

In agreement with studies in other areas, we found I_{tonic} in all our recordings from FS cells in M1. Our results show that I_{tonic} in FS cells is increased by 10 nM zolpidem, but that the opposite effect is seen at 30 nM. At these two concentrations, zolpidem has opposing effects on the power of beta oscillations in M1 and, given the strong relationship between FS cell function and network activity, it seems likely that the bidirectional effects on I_{tonic} and on network oscillatory power are related. The actions of flumazenil in blocking I_{tonic} and enhancement of oscillatory power in M1 further supports this interpretation. The benzodiazepine site has been implicated in modulation of neuronal network oscillations (Pálhalmi et al., 2004) and a zolpidem-sensitivity of I_{tonic} has also been reported in other areas, albeit at considerably higher concentrations (Semyanov et al., 2003; Gao and Smith, 2010). The actions of zolpidem at the low concentrations described above may involve subunit-specific effects. When tested on recombinant receptors, zolpidem displayed a high potency at α1-containing $GABA_A$ receptors (α1β2γ2, α1β3γ2: K_i = 20 nM). Zolpidem had medium potency at α2 and α3 containing $GABA_A$ receptors (e.g. α121γ2, α3β1γ2: K_i = 400 nM) and was ineffective at α5 subunit containing receptors (α5β3γ2, α5β2γ2: K_i 5000 nM) (Langer et al., 1992; Pritchett and Seeburg, 1990). The effects of very low concentrations of zolpidem on I_{tonic}, in our data strongly suggest that the $GABA_A$ receptors mediating the current in FS cells in M1 contain the α1 subunit (Pritchett and Seeburg, 1990; Langer et al., 1992; Crestani et al., 2000). This does not preclude the inclusion of δ subunits, believed to account for most of the I_{tonic} observed in other neurons (Brickley et al., 1996; Nusser and Mody, 2002; Belelli et al., 2005; Cope et al., 2005; Bright et al., 2007). Indeed, when we pre-applied the δ-subunit selective agonist, THIP, we found no occlusion of zolpidem induced augmentation of I_{tonic}, suggesting that non-desensitizing, δ-subunit containing receptors were not primarily involved in the response to zolpidem. This is consistent with our earlier experiments (Fig. 5) in which bicuculline blocked both the tonic current induced by 10 nM zolpidem and also a further, presumably zolpidem-insensitive, component.

Our data showed that application of zolpidem augmented an existing I_{tonic} in FS cells, indicated by the reduction of I_{tonic} beyond baseline by bicuculline. These data confirm previous reports (Semyanov et al., 2003) of a strong I_{tonic} at ambient GABA levels in FS cells in CA1 in the absence of uptake inhibitors. Moreover, the effect of flumazenil on both zolpidem-induced and baseline I_{tonic} suggests that in these cells the current depends on endogenous activation of the benzodiazepine site, as described recently by Christian et al. (2013).

That we found no effects of low concentrations of zolpidem on phasic inhibition indicates that the dual effects of zolpidem on neuronal network oscillations in M1 may be mediated via tonic inhibition alone. In support of this interpretation, Wulff et al. (2009) have recently reported that knockout of $GABA_A$ receptors on parvalbumin positive FS cells in hippocampus does not alter gamma activity, suggesting that extrasynaptic inhibitory drive may be more important than previously thought. The reduction in I_{tonic} seen with 30 nM zolpidem might be predicted to increase the number or effectiveness of FS cells participating in network activity, suggesting that the benzodiazepine-site may be involved in scaling the size of the active network.

What receptor states may underlie the behaviour of I_{tonic} in response to different degrees of benzodiazepine-site agonism? In our basic model, a population of closed, unbound receptors (U) exists in equilibrium with a population of closed, bound receptors (B_1 and B_2), and the latter population may transition between open, bound receptors (O_1 and O_2) and desensitized, receptors (D). There is also an open, unbound state (O_0). At low ambient [GABA], the lowest concentration of zolpidem (10 nM) has little effect on K_{off} and the probability of transition to O_1 and O_2 is low. However, the O_0 state is stabilized by effects of benzodiazepine binding on channel *gating* properties, which dominate over subtle effects on K_{off} (Bianchi, 2010), and this leads to increased charge transfer expressed macroscopically as enhancement of the tonic, unbound $GABA_AR$ conductance (Wlodarczyk et al., 2013). At higher concentrations of zolpidem (30–1000 nM), zolpidem begins to depress K_{off}, causing an apparent increase in *affinity* of the $GABA_AR$ for GABA and shifting the equilibrium toward an increase in C_b. The probability of moving from B into the O states at low ambient [GABA] remains low, as most receptors will be singly bound, and consequently the desensitized state, D, remains the highest affinity bound state. This leads to a shift in the equilibrium towards D, and macroscopic desensitization in the absence of significant increased charge transfer. Hence, at 10 nM, zolpidem acts to stabilize an open, unbound $GABA_AR$ through effects on *gating* leading to augmented I_{tonic}, and at 30–1000 nM, effects on *affinity* dominate and desensitization leads to a decreased macroscopic I_{tonic}. When [GABA] is raised artificially to 1000 nM most $GABA_AR$ are dual-bound, and hence effects on affinity dominate at all concentrations of zolpidem, because the population of receptors in C_b is large. Here, the equilibrium allows for transitions from B towards O and D, leading to augmented macroscopic currents and/or slow desensitization.

This model is further supported by the effects of flumazenil, application of which reveals a persistent GABA current even in the absence of zolpidem, suggesting that an endogenous benzodiazepine-mediated stabilization of the O_0 state exists in neocortical slices *in vitro* (Christian et al., 2013). Furthermore, when the proposed O_0 state is maximally augmented through prolonged incubation in 10 nM zolpidem at low ambient [GABA], the population of receptors sequestered into this state would be predicted to depress the rate and extent of maximal desensitization, since a smaller receptor population would be available to participate due to sequestration of receptors into the O_0 state. This is observed experimentally upon challenge of pre-incubated slices with 1 mM GABA (Fig. 11). This sequestration of receptors into a kinetically slow state presumably underlies the lack of effect of higher concentrations of zolpidem when applied subsequent to 10 nM zolpidem. By contrast, pre-incubation of slices with higher concentrations of zolpidem affects K_{off}, depressing the population of receptors in U, dominating subtle gating effects, and effectively depleting the pool of receptors in O_0. This pushes the equilibrium towards a high proportion of receptors in the B/O state, leading to return of maximal rates and extent of desensitization when GABA concentration is raised to mM levels.

4.3 Functional significance

The differential concentration-dependent effects of zolpidem on phasic and tonic inhibition in FS cells and consequent modulatory effects on oscillatory activity highlight the complex interplay

between these two inhibitory mechanisms. Indeed, the constitutively active $I_{tonic,}$ activated on FS cells by high affinity receptors may be a fundamental requirement for normal physiological functioning. It may act as a 'gatekeeper', having the ability to sculpt oscillatory power over a slower timescale than compared to phasic inhibition by thresholding the level of FS cell activity (Pavlov et al., 2009) and/or GABA before there is FS cell recruitment to an oscillation. Recent reports of 'endozepine' activity in the thalamus (Christian et al., 2013) confirm the importance of the benzodiazepine site in control of $GABA_A$ receptor function. Our data highlight how subtle alterations in both GABA and benzodiazepine site activation may confer radically different desensitization kinetics onto $GABA_A$ receptors, and how this may alter network activity. The origin of the GABA that activates receptors on FS cells is presumably input from other GABA neurons. Such disinhibitory interneuronal networks are currently a topic of great interest in understanding cortical circuit function (Lee et al., 2013; Pi et al., 2013 see also Klausberger et al., 2005).

The oscillations we have reported here are high beta/low gamma. Others have shown that oscillations *in vitro* depend linearly on temperature (Dickinson et al., 2003) and it is not possible to state with confidence that they relate to pathological beta activity as seen in Parkinson's, or indeed *in vivo* gamma activity as seen in healthy brain *in vivo*. However, our previous clinical studies in M1 have shown that pathological slow wave and beta frequency oscillations can be suppressed by low-dose zolpidem (Hall et al., 2010, 2014), effects which correlate with improved cognitive and motor function. It seems plausible that the effects of low-dose zolpidem on FS interneurons and the modulation of tonic inhibition may provide the mechanism underlying these clinical observations.

Author contributions

Experiments were conducted in the laboratories of GLW, GL and IMS. Conception and design of experiments, GLW; Collection, analysis and interpretation of data, EJP; Model simulations and analysis, CW, GL; article drafting GLW, EJP, RSGJ, IMS and revision GLW, EJP, SDH, CW, GL, RSGJ, IMS, NY. All authors approved the final version of the MS.

Acknowledgements

This work was supported by funding from a Warwick Impact Fund, a Warwick Research Development Fund (RD13301), the Birmingham Science City Research Alliance and The BBSRC (BB/G01227X/1).

Appendix A. Supplementary data

Supplementary data related to this article can be found at http://dx.doi.org/10.1016/j.neuropharm.2015.03.006.

References

Ali, A.B., Rossier, J., Staiger, J.F., Audinat, E., 2001. Kainate receptors regulate unitary IPSCs elicited in pyramidal cells by fast-spiking interneurons in the neocortex. J. Neurosci. 21, 2992–2999.
Ali, A.B., 2003. Involvement of post-synaptic kainate receptors during synaptic transmission between unitary connections in rat neocortex. Eur. J. Neurosci. 17, 2344–2350.
Bacci, A., Rudolph, U., Huguenard, J.R., Prince, D.A., 2003. Major differences in inhibitory synaptic transmission onto two neocortical interneuron subclasses. J. Neurosci. 23, 9664–9674.
Baker, S.N., Olivier, E., Lemon, R.N., 1997. Coherent oscillations in monkey motor cortex and hand muscle EMG show task-dependent modulation. J. Physiol. 501, 225–241.
Bai, D., Zhu, G., Pennefather, P., Jackson, M.F., MacDonald, J.F., Orser, B.A., 2001. Distinct functional and pharmacological properties of tonic and quantal inhibitory postsynaptic currents mediated by gamma-aminobutyric acid(A) receptors in hippocampal neurons. Mol. Pharmacol. 59, 814–824.
Bartos, M., Vida, I., Frotscher, M., Geiger, J.R., Jonas, P., 2001. Rapid signalling at inhibitory synapses in a dentate gyrus interneuron network. J. Neurosci. 21, 2687–2698.
Bartos, M., Vida, I., Frotscher, M., Meyer, A., Monyer, H., Geiger, J.R., Jonas, P., 2002. Fast synaptic inhibition promotes synchronized gamma oscillations in hippocampal interneuron networks. Proc. Natl. Acad. Sci. U. S. A. 99, 13222–13227.
Belelli, D., Peden, D.R., Rosahl, T.W., Wafford, K.A., Lambert, J.J., 2005. Extrasynaptic $GABA_A$ receptors of thalamocortical neurons: a molecular target for hypnotics. J. Neurosci. 25, 11513–11520.
Bianchi, M.T., Botzolakis, E.J., Lagrange, A.H., Macdonald, R.L., 2009. Benzodiazepine modulation of GABA(A) receptor opening frequency depends on activation context: a patch clamp and simulation study. Epilepsy Res. 85, 212–220.
Bianchi, M.T., 2010. Context dependent benzodiazepine modulation of GABA(A) receptor opening frequency. Curr. Neuropharmacol. 8, 10–17.
Brickley, S.G., Cull-Candy, S.G., Farrant, M., 1996. Development of a tonic form of synaptic inhibition in rat cerebellar granule cells resulting from persistent activation of GABAA receptors. J. Physiol. 497, 753–759.
Brickley, S.G., Revilla, V., Cull-Candy, S.G., Wisden, W., Farrant, M., 2001. Adaptive regulation of neuronal excitability by a voltage-independent potassium conductance. Nature 409, 88–92.
Bright, D.P., Aller, M.I., Brickley, S.G., 2007. Synaptic release generates a tonic GABA(A) receptor-mediated conductance that modulates burst precision in thalamic relay neurons. J. Neurosci. 27, 2560–2569.
Brown, P., 2003. The oscillatory nature of human basal ganglia activity; relationship to the pathophysiology of Parkinson's disease. Mov. Disord. 18, 357–363.
Brown, P., Mazzone, P., Oliviero, A., Altibrandi, M.G., Pilato, F., Tonali, P.A., Di, L.V., 2004. Effects of stimulation of the subthalamic area on oscillatory pallidal activity in Parkinson's disease. Exp. Neurol. 188, 480–490.
Canive, J.M., Lewine, J.D., Edgar, J.C., Davis, J.T., Torres, F., Roberts, B., 1996. Magnetoencephalographic assessment of spontaneous brain activity in schizophrenia. Psychopharmacol. Bull. 32, 741–750.
Cauli, B., Audinat, E., Lambolez, B., Angulo, M.C., Ropert, N., Tsuzuki, K., Hestrin, S., Rossier, J., 1997. Molecular and physiological diversity of cortical non-pyramidal cells. J. Neurosci. 17, 3894–3906.
Cheyne, D., Bells, S., Ferrari, P., Gaetz, W., Bostan, A.C., 2008. Self-paced movements induce high-frequency gamma oscillations in primary motor cortex. Neuroimage 42, 332–342.
Christian, C.A., Herbert, A.G., Holt, R.L., Peng, K., Sherwood, K.D., Pangratz-Fuehrer, S., Rudolph, U., Huguenard, J.R., 2013. Endogenous positive allosteric modulation of GABA(A) receptors by diazepam binding inhibitor. Neuron 78, 1063–1074.
Clarkson, A.N., Huang, B.S., Macisaac, S.E., Mody, I., Carmichael, S.T., 2010. Reducing excessive GABA-mediated tonic inhibition promotes functional recovery after stroke. Nature 468, 305–309.
Cobb, S.R., Buhl, E.H., Halasy, K., Paulsen, O., Somogyi, P., 1995. Synchronization of neuronal activity in hippocampus by individual GABAergic interneurons. Nature 378, 75–78.
Cope, D.W., Halbsguth, C., Karayannis, T., Wulff, P., Ferraguti, F., Hoeger, H., Leppa, E., Linden, A.M., Oberto, A., Ogris, W., Korpi, E.R., Sieghart, W., Somogyi, P., Wisden, W., Capogna, M., 2005. Loss of zolpidem efficacy in the hippocampus of mice with the $GABA_A$ receptor gamma2 F77I point mutation. Eur. J. Neurosci. 21, 3002–3016.
Crestani, F., Martin, J.R., Mohler, H., Rudolph, U., 2000. Mechanism of action of the hypnotic zolpidem in vivo. Br. J. Pharmacol. 131, 1251–1254.
Croft, W., Hill, C., McCann, E., Bond, M., Esparza-Franco, M., Bennett, J., Rand, D., Davey, J., Ladds, G., 2013. A physiologically required G protein-coupled receptor (GPCR)-regulator of G protein signaling (RGS) interaction that compartmentalizes RGS activity. J. Biol. Chem. 288, 27327–27342.
Dickinson, R., Awaiz, S., Whittington, M.A., Lieb, W.R., Franks, N.P., 2003. The effects of general anaesthetics on carbachol-evoked gamma oscillations in the rat hippocampus in vitro. Neuropharmacology 44 (7), 864–872.
Farrant, M., Nusser, Z., 2005. Variations on an inhibitory theme: phasic and tonic activation of GABAA receptors. Nat. Rev. Neurosci. 6, 215–229.
Fisahn, A., Pike, F.G., Buhl, E.H., Paulsen, O., 1998. Cholinergic induction of network oscillations at 40 Hz in the hippocampus in vitro. Nature 394, 186–189.
Ford, J.M., Krystal, J.H., Mathalon, D.H., 2007. Neural synchrony in schizophrenia: from networks to new treatments. Schizophr. Bull. 3, 848–852.
Gao, H., Smith, B.N., 2010. Zolpidem modulation of phasic and tonic GABA currents in the rat dorsal motor nucleus of the vagus. Neuropharmacology 58, 1220–1227.
Glaze, D.G., 1990. Drug effects. In: Daly, D.D., Pedley, T.A. (Eds.), Current Practice of Clinical Electroencephalography, second ed. Raven Press, New York, pp. 489–512.
Greenblatt, D.J., Legangneux, E., Harmatz, J.S., Weinling, E., Freeman, J., Rice, K., Zammit, G.K., 2006. Dynamics and kinetics of a modified-release formulation of zolpidem: comparison with immediate-release standard zolpidem and placebo. J. Clin. Pharmacol. 46, 1469–1480.
Hall, S.D., Yamawaki, N., Fisher, A.E., Clauss, R.P., Woodhall, G.L., Stanford, I.M., 2010. GABA(A) alpha-1 subunit mediated desynchronization of elevated low frequency oscillations alleviates specific dysfunction in stroke-a case report. Clin. Neurophysiol. 121, 549–555.
Hall, S.D., Prokic, E.J., McAllister, C.J., Ronnqvist, Q.C., Williams, A.C., Yamawaki, N., Witton, C., Woodhall, G.L., Stanford, I.M., 2014. GABA-mediated changes in

inter-hemispheric beta frequency activity in early-stage Parkinson's disease. Neuroscience 281C, 68–76.
Jones, M.V., Sahara, Y., Dzubay, J.A., Westbrook, G.L., 1998. Defining affinity with the $GABA_A$ receptor. J. Neurosci. 18, 8590–8604.
Jones, M.V., Westbrook, G.L., 1995. Desensitized states prolong $GABA_A$ channel responses to brief agonists pulses. Neuron 15, 181–191.
Karayannis, T., Elfant, D., Huerta-Ocampo, I., Teki, S., Scott, R.S., Rusakov, D.A., Jones, M.V., Capogna, M., 2010. Slow GABA transient and receptor desensitization shape synaptic responses evoked by hippocampal neurogliaform cells. J. Neurosci. 30, 9898–9909.
Kawaguchi, Y., 1995. Physiological subgroups of non-pyramidal cells with specific morphological characteristics in layer II/III of rat frontal cortex. J. Neurosci. 15, 2638–2655.
Kawaguchi, Y., Kubota, K., 1997. GABAergic cell subtypes and their synaptic connections in rat frontal cortex. Cereb. Cortex 7, 476–486.
Klausberger, T., Marton, L.F., O'Neill, J., Huck, J.H., Dalezios, Y., Fuentealba, P., Suen, W.Y., Papp, E., Kaneko, T., Watanabe, M., Csicsvari, J., Somogyi, P., 2005. Complementary roles of cholecystokinin- and parvalbumin-expressing GABAergic neurons in hippocampal network oscillations. J. Neurosci. 25, 9782–9793.
Koniaris, E., Drimala, P., Sotiriou, E., Papatheodoropoulos, C., 2011. Different effects of zolpidem and diazepam on hippocampal sharp wave-ripple activity in vitro. Neuroscience 175, 224–234.
Kuhn, A.A., Kupsch, A., Schneider, G.H., Brown, P., 2006. Reduction in subthalamic 8–35 Hz oscillatory activity correlates with clinical improvement in Parkinson's disease. Eur. J. Neurosci. 23, 1956–1960.
Langer, S.Z., Faure-Halley, C., Seeburg, P., Graham, D., Arbilla, S., 1992. The selectivity of zolpidem and alpidem for the alpha1-subunit of the $GABA_A$ receptor. Eur. Neuropsychopharmacol. 2, 232–234.
Lee, S., Kruglikov, I., Huang, Z.J., Fishell, G., Rudy, B., 2013. A disinhibitory circuit mediates motor integration in the somatosensory cortex. Nat. Neurosci. 16, 1662–1670.
Mann, E.O., Mody, I., 2010. Control of hippocampal gamma oscillation frequency by tonic inhibition and excitation of interneurons. Nat. Neurosci. 13, 205–212.
Manseau, F., Marinelli, S., Méndez, P., Schwaller, B., Prince, D.A., Huguenard, J.R., Bacci, A., 2010. Desynchronization of neocortical networks by asynchronous release of GABA at autaptic and synaptic contacts from fast-spiking interneurons. PLoS Biol. 8 (9), e1000492.
McKernan, R.M., Wafford, K., Quirk, K., Hadingham, K.L., Harley, E.A., Ragan, C.I., Whiting, P.J., 1995. The pharmacology of the benzodiazepine site of the GABA-A receptor is dependent on the type of gamma-subunit present. J. Recept. Signal Transduct. Res. 15 (1–4), 173–183.
Meera, P., Wallner, M., Otis, T.S., 2011. Molecular basis for the high THIP/gaboxadol sensitivity of extrasynaptic GABA(A) receptors. J. Neurophysiol. 106, 2057–2064.
Mellor, J.R., Randall, A.D., 1997. Frequency-dependent actions of benzodiazepines on $GABA_A$ receptors in cultured murine cerebellar granule cells. J. Physiol. 503, 353–369.
Murthy, V.N., Fetz, E.E., 1992. Coherent 25- to 35-Hz oscillations in the sensorimotor cortex of awake behaving monkeys. Proc. Natl. Acad. Sci. U. S. A. 89, 5670–5674.
Nusser, Z., Sieghart, W., Somogyi, P., 1998. Segregation of different $GABA_A$ receptors to synaptic and extrasynaptic membranes of cerebellar granule cells. J. Neurosci. 18, 1693–1703.
Nusser, Z., Mody, I., 2002. Selective modulation of tonic and phasic inhibitions in dentate gyrus granule cells. J. Neurophysiol. 87, 2624–2628.
Olubodun, J.O., Ochs, H.R., von Moltke, L.L., Roubenoff, R., Hesse, L.M., Harmatz, J.S., Shader, R.I., Greenblatt, D.J., 2003. Pharmacokinetic properties of zolpidem in elderly and young adults: possible modulation by testosterone in men. Br. J. Clin. Pharmacol. 56, 297–304.
Pálhalmi, J., Paulsen, O., Freund, T.F., Hájos, N., 2004. Distinct properties of carbachol- and DHPG-induced network oscillations in hippocampal slices. Neuropharmacology 47, 381–389.
Pakhotin, P.I., Pakhotina, I.D., Andreev, A.A., 1997. Functional stability of hippocampal slices after treatment with cyclooxygenase inhibitors. Neuroreport 8, 1755–1759.
Pavlov, I., Savtchenko, L.P., Kullmann, D.M., Semyanov, A., Walker, M.C., 2009. Outwardly rectifying tonically active GABAA receptors in pyramidal cells modulate neuronal offset, not gain. J. Neurosci. 29, 15341–15350.
Petrini, E.M., Nieus, T., Ravasenga, T., Succol, F., Guazzi, S., Benfenati, F., Barberis, A., 2011. Influence of GABAAR monoliganded states on GABAergic responses. J. Neurosci. 31, 1752–1761.
Pi, H.J., Hangya, B., Kvitsiani, D., Sanders, J.I., Huang, Z.J., Kepecs, A., 2013. Cortical interneurons that specialize in disinhibitory control. Nature 503, 521–524.
Poza, J., Hornero, R., Abasolo, D., Fernandez, A., Escudero, J., 2007. Analysis of spontaneous MEG activity in patients with Alzheimer's disease using spectral entropies. In: Conf. Proc. IEEE Eng. Med. Biol. Soc, pp. 6180–6183.
Pritchett, D.B., Seeburg, P.H., 1990. $GABA_A$ receptor alpha5-subunit creates novel type II benzodiazepine receptor pharmacology. J. Neurochem. 545, 1802–1804.
Salvà, P., Costa, J., 1995. Clinical pharmacokinetics and pharmacodynamics of zolpidem. Therapeutic implications. Clin. Pharmacokinet. 29, 142–153.
Semyanov, A., Walker, M.C., Kullmann, D.M., 2003. GABA uptake regulates cortical excitability via cell type-specific tonic inhibition. Nat. Neurosci. 6, 484–490.
Semyanov, A., Walker, M.C., Kullmann, D.M., Silver, R.A., 2004. Tonically active GABA A receptors: modulating gain and maintaining the tone. Trends Neurosci. 27, 262–269.
Tecchio, F., Zappasodi, F., Pasqualetti, P., Tombini, M., Caulo, M., Ercolani, M., Rossini, P.M., 2006. Long-term effects of stroke on neuronal rest activity in rolandic cortical areas. J. Neurosci. Res. 83, 1077–1087.
Thomson, A.M., Bannister, A.P., Hughes, D.I., Pawelzik, H., 2000. Differential sensitivity to Zolpidem of IPSPs activated by morphologically identified CA1 interneurons in slices of rat hippocampus. Eur. J. Neurosci. 12, 425–436.
Traub, R.D., Whittington, M.A., Colling, S.B., Buzsaki, G., Jefferys, J.G.R., 1996. Analysis of gamma rhythms in the rat hippocampus in vitro and in vivo. J. Physiol. 493, 471–484.
Traub, R.D., Cunningham, M.O., Gloveli, T., LeBeau, F.E., Bibbig, A., Buhl, E.H., Whittington, M.A., 2003. GABA-enhanced collective behavior in neuronal axons underlies persistent gamma-frequency oscillations. Proc. Natl. Acad. Sci. U. S. A. 100, 11047–11052.
Whittington, M.A., Traub, R.D., Jefferys, J.G.R., 1995. Synchronized oscillations in interneuron networks driven by metabotropic glutamate receptor activation. Nature 373, 612–615.
Wlodarczyk, A.I., Sylantyev, S., Herd, M.B., Kersanté, F., Lambert, J.J., Rusakov, D.A., Linthorst, A.C., Semyanov, A., Belelli, D., Pavlov, I., Walker, M.C., 2013. GABA-independent $GABA_A$ receptor openings maintain tonic currents. J. Neurosci. 33, 3905–3914.
Wulff, P., Ponomarenko, A.A., Bartos, M., Korotkova, T.M., Fuchs, E.C., Bähner, F., Both, M., Tort, A.B., Kopell, N.J., Wisden, W., Monyer, H., 2009. Hippocampal theta rhythm and its coupling with gamma oscillations require fast inhibition onto parvalbumin-positive interneurons. Proc. Natl. Acad. Sci. U. S. A. 106 (9), 3561–3566.
Yamada, J., Furukawa, T., Ueno, S., Yamamoto, S., Fukuda, A., 2007. Molecular basis for the $GABA_A$ receptor-mediated tonic inhibition in rat somatosensory cortex. Cereb. Cortex 17, 1782–1787.
Yamawaki, N., Stanford, I.M., Hall, S.D., Woodhall, G.L., 2008. Pharmacologically induced and stimulus evoked rhythmic neuronal oscillatory activity in the primary motor cortex in vitro. Neuroscience 151, 386–395.